THE JOURNAL OF BIOLOGICAL CHEMISTRY VOL. 290, NO. 3, pp. 1654–1663, January 16, 2015

Distinct Roles of *N*-Glycosylation at Different Sites of Corin in Cell Membrane Targeting and Ectodomain Shedding*

Received for publication, August 21, 2014, and in revised form, November 16, 2014 Published, JBC Papers in Press, December 1, 2014, DOI 10.1074/jbc.M114.606442

Hao Wang[‡§], Tiantian Zhou[¶], Jianhao Peng[‡], Ping Xu[‡1], Ningzheng Dong[¶], Shenghan Chen[‡], and Qingyu Wu[‡§¶2]

From the [‡]Department of Molecular Cardiology, Lerner Research Institute, Cleveland Clinic, Cleveland, Ohio 44195, the [§]Department of Chemistry, Cleveland State University, Cleveland, Ohio 44115, and the [¶]Cyrus Tang Hematology Center and Collaborative Innovation Center of Hematology, Soochow University, Suzhou 215123, China

Background: Corin is a transmembrane protease containing 19 predicted *N*-glycosylation sites.
Results: Corin mutants lacking individual *N*-glycosylation sites were studied for their biosynthesis and processing.
Conclusion: *N*-Glycosylation at different sites plays distinct roles in preventing ectodomain shedding and promoting cell surface targeting and zymogen activation.
Significance: The results are important for understanding how corin expression and activity are regulated.

Corin is a membrane-bound protease essential for activating natriuretic peptides and regulating blood pressure. Human corin has 19 predicted *N*-glycosylation sites in its extracellular domains. It has been shown that *N*-glycans are required for corin cell surface expression and zymogen activation. It remains unknown, however, how *N*-glycans at different sites may regulate corin biosynthesis and processing. In this study, we examined corin mutants, in which each of the 19 predicted *N*-glycosylation sites was mutated individually. By Western analysis of corin proteins in cell lysate and conditioned medium from transfected HEK293 cells and HL-1 cardiomyocytes, we found that *N*-glycosylation at Asn-80 inhibited corin shedding in the juxtamembrane domain. Similarly, *N*-glycosylation at Asn-231 protected corin from autocleavage in the frizzled-1 domain. Moreover, *N*-glycosylation at Asn-697 in the scavenger receptor domain and at Asn-1022 in the protease domain is important for corin cell surface targeting and zymogen activation. We also found that the location of the *N*-glycosylation site in the protease domain was not critical. *N*-Glycosylation at Asn-1022 may be switched to different sites to promote corin zymogen activation. Together, our results show that *N*-glycans at different sites may play distinct roles in regulating the cell membrane targeting, zymogen activation, and ectodomain shedding of corin.

Corin is a type II transmembrane serine protease that regulates salt-water balance and blood pressure (1, 2). Corin is expressed primarily in the heart (3–5), where it activates atrial natriuretic peptide (ANP),[3] which promotes sodium excretion and vessel relaxation, thereby reducing blood volume and pressure (6–10). Variants and mutations in the genes encoding corin and ANP have been found in patients with hypertension and heart disease (11–19), supporting the importance of the corin and ANP pathway in maintaining normal blood pressure and cardiac function. Corin and ANP may also act locally in the pregnant uterus to promote trophoblast invasion and spiral artery remodeling (20–23), which are critical for regulating maternal blood pressure. Genetic mutations that impair corin function have been identified in patients with pregnancy-induced hypertension (21, 24).

Human corin is a polypeptide of 1,042 amino acids, consisting of an N-terminal transmembrane domain and an extracellular region with two frizzled (Fz) domains, eight LDL receptor (LDLR) repeats, one scavenger receptor domain, and a C-terminal trypsin-like protease domain (2, 3). The calculated mass for the full-length human corin is ~116 kDa (2, 3). On Western blots, human corin expressed in HEK293 cells appeared as bands of ~170–200 kDa (25, 26). Human corin has 19 predicted *N*-glycosylation sites. *N*-Glycans attached to these sites may explain the difference between the calculated and the observed corin protein masses (2, 3). In glycosidase digestion experiments, human corin was shown to contain abundant *N*-glycans but no detectable *O*-glycans or sialic acids (25). *N*-Glycans also have been detected in mouse, rat, and dog corin proteins (25, 27–29).

In cells, corin is synthesized as a one-chain zymogen with no detectable catalytic activity (1). Upon reaching the cell surface, corin is converted to a two-chain active protease by cleavage at a conserved activation site. To date, the enzyme(s) responsible for corin activation remain poorly defined. It has been shown that a protein motif in the corin cytoplasmic tail facilitates intracellular trafficking and cell surface expression (26). In addition, *N*-glycans have been found to be important in corin cell surface targeting and zymogen activation. In transfected

* This work was supported, in whole or in part, by National Institutes of Health Grants HL089298 and HD064634. This work was also supported by National Natural Science Foundation of China Grant 81370718, a grant from the Priority Academic Program Development of Jiangsu Higher Education Institutions, and Danish-Chinese Center for Protease and Cancer Grant 31161130356.

[1] Present address: Peking University Shenzhen Hospital, Shenzhen, Guangdong 518036, China.
[2] To whom correspondence should be addressed: Molecular Cardiology, Cleveland Clinic, 9500 Euclid Ave., Cleveland, OH 44195. Tel.: 216-444-4351; Fax: 216-445-8204; E-mail: wuq@ccf.org.

[3] The abbreviations used are: ANP, atrial natriuretic peptide; ADAM, a disintegrin and metalloprotease; Fz, frizzled; HEK, human embryonic kidney; LDLR, LDL receptor.

HEK293 cells and cultured cardiomyocytes, blocking *N*-glycosylation by tunicamycin prevented corin expression and activation on the cell surface (25, 27). Similar roles of *N*-glycosylation in regulating cell surface expression and zymogen activation have been reported in other type II transmembrane serine proteases, such as enteropeptidase (30), matriptase (31), and matriptase-2 (32), which are involved in food digestion, epithelial function, and iron metabolism, respectively (33, 34).

In this study, we tested the hypothesis that *N*-glycosylation at individual sites may have distinct roles in regulating biosynthesis and post-translational processing of corin. We generated corin mutants, in which each of the 19 predicted *N*-glycosylation sites was mutated individually. The mutants were expressed in HEK293 cells and HL-1 cardiomyocytes. The expressed corin proteins were analyzed by Western blotting, immunostaining, and flow cytometry. Our results indicate that *N*-glycans at individual sites have different roles in regulating corin cell membrane targeting, zymogen activation, and ectodomain shedding.

EXPERIMENTAL PROCEDURES

Cell Culture—HEK293 cells were grown in Dulbecco's modified Eagle's medium with 10% fetal bovine serum (FBS). Murine HL-1 cardiomyocytes were provided by William Claycomb (Louisiana State University) and cultured in Claycomb medium (Sigma) with 10% FBS and 4 mM L-glutamine, as described previously (26, 35). The cells were cultured at 37 °C in humidified incubators with 5% CO_2 and 95% air.

Plasmid Constructs—Plasmids for human wild-type (WT) corin, activation cleavage site mutant R801A, and active site mutant S985A were described previously (36). Plasmids expressing corin mutants N80Q, N104Q, N135Q, N141Q, N231Q, N245Q, N251Q, N305Q, N320Q, N376Q, N413Q, N446Q, N451Q, N469Q, N567Q, N651Q, N697Q, N761Q, and N1022Q were generated by PCR-based mutagenesis using WT corin plasmid as a template. Additional plasmids were made to express corin mutants N77 (F77N/K78G/N80Q), N77c (F77N/K78G/S79A/N80Q), N83 (N80Q/E83N/P84G/L85S), N83c (N80Q/E83N/P84G), N231Q/S985A, S903N, S903N/N1022Q, T963N/N1022Q, and S975N/N1022Q (see Figs. 5*A*, 6*A*, and 8*A*). All corin proteins expressed by these plasmids had a C-terminal V5 tag for protein detection.

Expression and Analysis of Corin Proteins—Plasmids were transfected into HEK293 and HL-1 cells using FuGENE (Promega) or Lipofectamine 2000 (Invitrogen). Conditioned medium was collected after 48–60 h. Expressed corin proteins were immunoprecipitated using an anti-V5 antibody (Invitrogen). The cells were lysed in a buffer with 50 mM Tris-HCl (pH 8.0), 150 mM NaCl, 1% Nonidet P-40 (v/v), and a protease inhibitor mixture (1:100; Sigma). Protein samples were denatured in a buffer with (reducing) or without (non-reducing) 2.5% β-mercaptoethanol and separated by SDS-PAGE. A horseradish peroxidase-conjugated anti-V5 antibody was used to detect corin proteins on Western blots. X-ray films exposed to the Western blots were analyzed by densitometry, and the bands representing corin fragments were analyzed by the Quantity One software (Bio-Rad).

Immunostaining—HEK293 cells expressing corin proteins were cultured on glass slides in 8-well plates (Falcon, BD Biosciences) under the conditions described above. The cells were fixed with 3% paraformaldehyde in phosphate-buffered saline (PBS) for 15 min and incubated with PBS with 1% bovine serum albumin for 30 min, followed with an anti-V5 antibody for 1 h. An Alexa Fluor 594-labeled donkey anti-mouse antibody (Invitrogen) was used as a secondary detection antibody. The slides were mounted in a medium with DAPI (Vector Laboratories). The stained cells were examined under a light microscope (Leica DM2500).

Pro-ANP Processing—Human pro-ANP was expressed in stably transfected HEK293 cells. The conditioned medium containing pro-ANP was collected and incubated with HEK293 cells expressing corin WT or mutants at 37 °C for 30 min. Pro-ANP and ANP in the conditioned medium were immunoprecipitated and analyzed by SDS-PAGE and Western blotting, as described previously (26).

Analysis of Cell Surface Proteins—HEK293 cells expressing corin were labeled with 200 μM sulfo-NHS-SS-biotin (Pierce) in PBS at 4 °C for 5 min. The reaction was stopped by adding 100 mM glycine. The cells were lysed and the lysate was incubated with NeutrAvidin agarose beads (Pierce) at room temperature for 2 h. The beads were washed three times with PBS and boiled in a sample buffer with 2.5% β-mercaptoethanol. The eluted proteins were analyzed by SDS-PAGE and Western blotting.

Flow Cytometry—Cell surface corin expression in intact cells was analyzed by flow cytometry (26). Transfected HEK293 cells expressing corin were incubated with an anti-V5 antibody and an FITC-conjugated secondary antibody. Life-cell gating was performed with pyridinium iodide (Sigma). Data were collected with a flow cytometer (FACSCalibur, BD Biosciences) and analyzed by the CellQuest software.

Glycosidase Digestion—Cell lysates from HEK293 cells expressing corin proteins were prepared, denatured, and incubated in a buffer containing peptide-*N*-glycosidase F (Promega). After 2 h at 37 °C, corin proteins were analyzed by SDS-PAGE and Western blotting.

Molecular Modeling—Three-dimensional models of the human corin Fz1 domain and the serine protease domain were created using a computer-based modeling program (SWISS-MODEL) (37). The amino acid sequences of the human corin Fz1 and the protease domains were submitted to a fully automated server (SWISS-MODEL), which generated three-dimensional models based on crystal structures of homologous proteins. The model inspection and image generation were done with the PyMOL program (Schroedinger, LLC, New York), as described previously (24).

Statistical Analysis—Analysis was performed with Prism software (GraphPad). Comparisons between two groups were done using Student's *t* test. Comparisons among three or more groups were done using analysis of variance followed by a post hoc analysis. A p value of <0.05 was considered to be statistically significant.

RESULTS

Corin Activation in N-Glycosylation Site Mutants—Human corin is activated at Arg-801 (Fig. 1*A*). After activation, the protease domain remains membrane-bound via a disulfide bond. As reported previously (26), the cleaved protease domain frag-

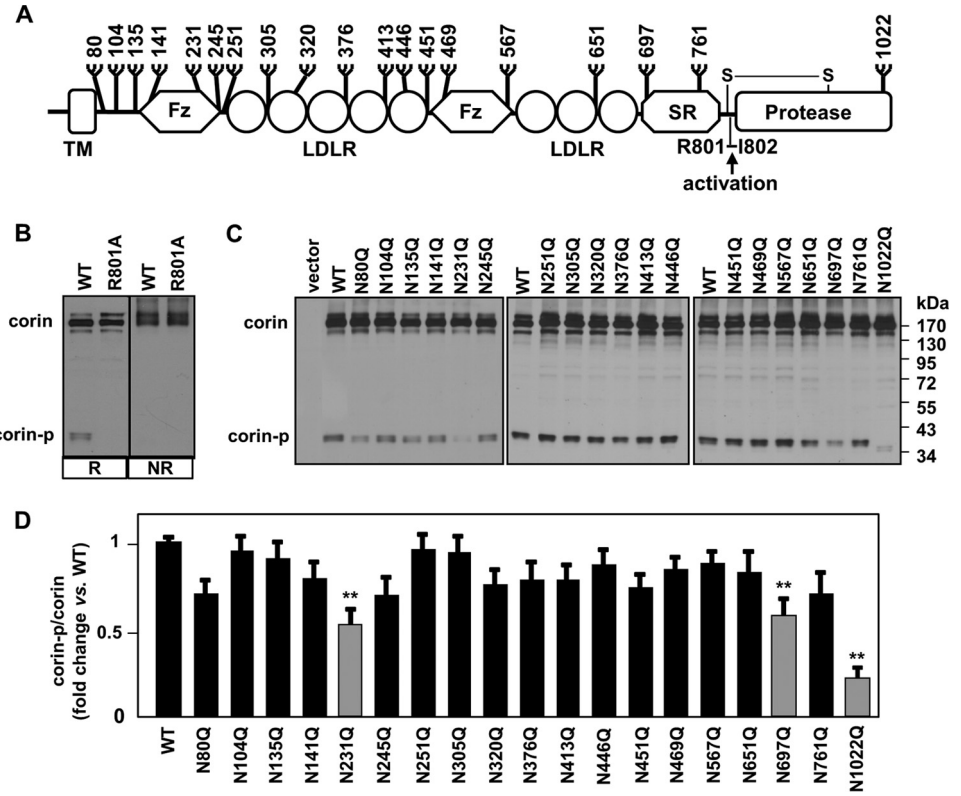

FIGURE 1. **Zymogen activation of corin WT and *N*-glycosylation site mutants.** *A*, human corin domains and *N*-glycosylation sites. The transmembrane (*TM*), frizzled (*Fz*), LDL receptor (*LDLR*), scavenger receptor (*SR*), and serine protease (*Protease*) domains of corin are illustrated. An *arrow* indicates the activation cleavage site between Arg-801 (*R801*) and Ile-802 (*I802*). The disulfide bond (*S-S*) that links the propeptide and the protease domains is shown. Locations of 19 predicted *N*-glycosylation sites are indicated. *B*, Western blotting analysis of corin WT and R801A mutant in transfected HEK293 cells under reducing (*R*) and non-reducing (*NR*) conditions. The activation-cleaved corin protease domain fragment (*corin-p*) is indicated. *C*, Western blotting analysis of corin WT and *N*-glycosylation site mutants in transfected HEK293 cells under reducing conditions. *D*, ratios of corin-p *versus* corin bands, as estimated by densitometric analysis of Western blots. Data are means ± S.E. (*error bars*) from nine independent experiments. **, $p < 0.01$ *versus* WT.

ment (*corin-p*) migrated as an ~40 kDa band on Western blots under reducing conditions (Fig. 1*B*, *left*). Under non-reducing conditions, activated and zymogen corin molecules were indistinguishable (Fig. 1*B*, *right*). In the corin R801A mutant that lacked the activation site, the corin-p fragment was absent (Fig. 1*B*, *left*). Because corin is activated on the cell surface (26), the corin-p band serves as an indicator for corin cell surface targeting and activation.

To examine the importance of *N*-glycosylation at individual sites in corin biosynthesis and processing, we expressed corin mutants, in which each Asn at the 19 predicted *N*-glycosylation sites was mutated individually (Fig. 1*A*). In transfected HEK293 cells, corin WT and mutant proteins were expressed at similar levels, as indicated by comparable intensities of the top corin bands (*corin*) on Western blots under reducing conditions (Fig. 1*C*). The activated corin-p band was detected in each of the corin samples, although the levels were lower in mutants N80Q, N231Q, N697Q, and N1022Q (Fig. 1*C*). The ratio of corin-p *versus* zymogen bands in N231Q, N697Q, and N1022Q mutants decreased to 53 ± 9, 57 ± 11, and 22 ± 7% of WT, respectively ($n = 9$, all p values <0.01 *versus* WT) (Fig. 1*D*). The ratio in mutant N80Q also decreased (71 ± 8% of WT), but the reduction was not statistically significant (Fig. 1*D*). In mutant N1022Q, the corin-p band migrated faster than that in the other samples (Fig. 1*C*, *right*) because the fragment from the mutant lacked *N*-glycans, whereas the Asn-1022 *N*-glycosylation site was preserved in the other mutants and WT corin. The results indicate that *N*-glycosylation at Asn-231, -697, and -1022, but not at the other sites, is important for corin cell surface expression and zymogen activation.

Corin Shedding in N-Glycosylation Site Mutants—It has been reported that activated corin undergoes proteolytic shedding, producing three fragments of ~180, ~160, and ~100 kDa, respectively (36). The ~180-kDa fragment was shown to be cleaved by a disintegrin and metalloprotease-10 (ADAM10), whereas the ~160- and ~100-kDa fragments were produced by corin autocleavage (36) (Fig. 2*A*).

We examined corin fragments in the conditioned medium from the transfected cells. Consistent with the previous finding (36), three bands of ~180, ~160, and ~100 kDa were detected in WT samples, whereas only the ~180 kDa band was detected in mutant R801A that was catalytically inactive (Fig. 2*B*). In mutant N80Q, the level of the ~180 kDa band increased significantly (486 ± 39% of WT, $n = 6$, $p < 0.01$) (Fig. 2, *C* and *D*). In mutant N231Q, the level of the ~160 kDa band, but not that of the ~180 or ~100 kDa band, increased (159 ± 14% of WT, $n = 6$, $p < 0.05$) (Fig. 2, *C* and *E*). In contrast, in N697Q and N1022Q mutants, levels of all three bands decreased (30 ± 6% of WT for N697Q, $p < 0.05$; 20 ± 5% of WT for N1022Q, $p < 0.01$; $n = 6$) (Fig. 2, *C* and *F*). The results indicate that *N*-glycans at Asn-80, -231, -697, and -1022 may alter corin ectodomain shedding and/or cell surface expression.

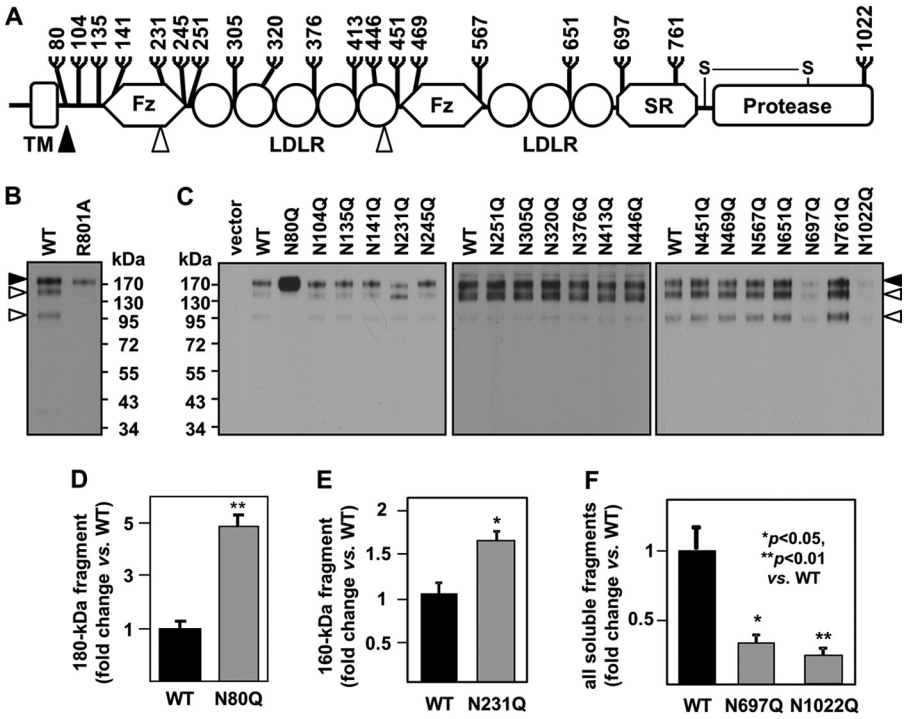

FIGURE 2. **Ectodomain shedding of corin WT and *N*-glycosylation site mutants.** *A*, ADAM10-mediated shedding (*filled arrowhead*) and corin autocleavage (*open arrowheads*) sites. Shown is Western blotting analysis of corin fragments in the conditioned medium from HEK293 cells expressing corin WT, R801A mutant (*B*), and *N*-glycosylation site mutants (*C*). Three fragments of ~180, ~160, and ~100 kDa, respectively, are indicated by *arrowheads*. *D*, relative levels of the ~180-kDa fragment in samples from WT and N80Q mutant. *E*, relative levels of the ~160-kDa fragment in samples from WT and N231Q mutant. *F*, relative levels of all three fragments in samples from WT and the N697Q and N1022Q mutants. Values are means ± S.D. (*error bars*) from six independent experiments. *, $p < 0.05$; **, $p < 0.01$ *versus* WT in each group.

Analysis of Corin Mutants in HL-1 Cells—Corin is expressed primarily in cardiomyocytes (2–4). We also expressed and analyzed the corin mutants in HL-1 cardiomyocytes. Western blotting analysis showed reduced corin zymogen activation in N80Q, N231Q, N697Q, and N1022Q mutants (Fig. 3*A*, *top*). The ratio of corin-p *versus* zymogen bands in these mutants was 60 ± 9, 55 ± 18, 57 ± 7, and 19 ± 7% of WT, respectively ($n = 5$, all p values <0.01 *versus* WT) (Fig. 3*B*).

In the conditioned medium from the transfected HL-1 cells, the level of the ~180 kDa band increased in N80Q mutant (432 ± 27% of WT, $n = 3$, $p < 0.01$), whereas the level of the ~160 kDa band increased in N231Q mutant (201 ± 38% of WT, $n = 3$, $p < 0.01$) (Fig. 3, *A* (*bottom*), *C*, and *D*). In contrast, levels of all three bands decreased in N687Q and N1022Q mutants (31 ± 11 and 25 ± 5% of WT, respectively; $n = 3$; both p values <0.01) (Fig. 3, *A* (*bottom*) and *E*). These results are consistent with the findings from the transfected HEK293 cells.

Pro-ANP Processing Activity—We next examined the activity of the corin mutants. In a pro-ANP processing assay, reduced activities were observed in N231Q, N697Q, and N1022Q mutants (54 ± 7, 61 ± 8, and 42 ± 13% of WT, respectively; $n = 7$; $p < 0.05$ for N697Q; $p < 0.01$ for N231Q and N1022Q *versus* WT) (Fig. 4, *A* and *B*). The activity of N80Q, N567Q, and N761Q mutants was not statistically different from that of WT ($n = 7$, p values >0.05), although the activity of N80Q mutant appeared to be lower. As a negative control, R801A mutant had little activity in this assay (Fig. 4*A*).

N-Glycosylation at Asn-80 Protected Corin from ADAM-mediated Shedding—The high level of the ~180-kDa fragment, which was cleaved by ADAM10 (36), in N80Q mutant suggested that *N*-glycans at Asn-80 may protect corin from proteolytic shedding at this site. To verify this hypothesis, we designed two additional mutants, N77 and N83, in which the *N*-glycosylation site at residue 80 was abolished and a new site was created at residue 77 or 83 (Fig. 5*A*). Two respective control mutants, N77c and N83c, also were made, in which Asn residue 77 or 83 was not followed by the consensus *N*-glycosylation site sequence (N*X*(S/T), where *X* can be any amino acid but Pro) (Fig. 5*A*).

In Western analysis, WT and mutant corin levels in the transfected HEK293 cells were similar (Fig. 5*B*, *bottom*). In the conditioned medium, levels of the ~180-kDa band in N77 and N83 mutants were similar to that in WT (93 ± 26 and 120 ± 38% of WT, respectively; $n = 6$; p values >0.05). In N80Q mutant and two additional control mutants, N77c and N83c, the levels of this band were higher (426 ± 41, 469 ± 56, and 407 ± 15% of WT, respectively; $n = 6$; all p values <0.01) (Fig. 5, *B* and *C*), indicating that *N*-glycans at or near residue 80 may protect corin from proteolytic shedding in the juxtamembrane domain.

N-Glycosylation at Asn-231 Protected Corin from Autocleavage in the Fz1 Domain—As reported previously, the ~160-kDa fragment was from corin autocleavage at residue Arg-164 in the Fz1 domain (36). The high level of the ~160 kDa band from N231Q mutant (Fig. 2, *C* and *E*) suggested that *N*-glycans at Asn-231 may block corin autocleavage in the Fz1 domain (Fig. 6*A*). To understand the spatial position of Arg-164 and Asn-231 in the Fz1 domain, we created a computer-based three-dimensional model, which showed that Arg-164 and Asn-231 were surface-exposed and located at a distance of ~30 Å apart (Fig.

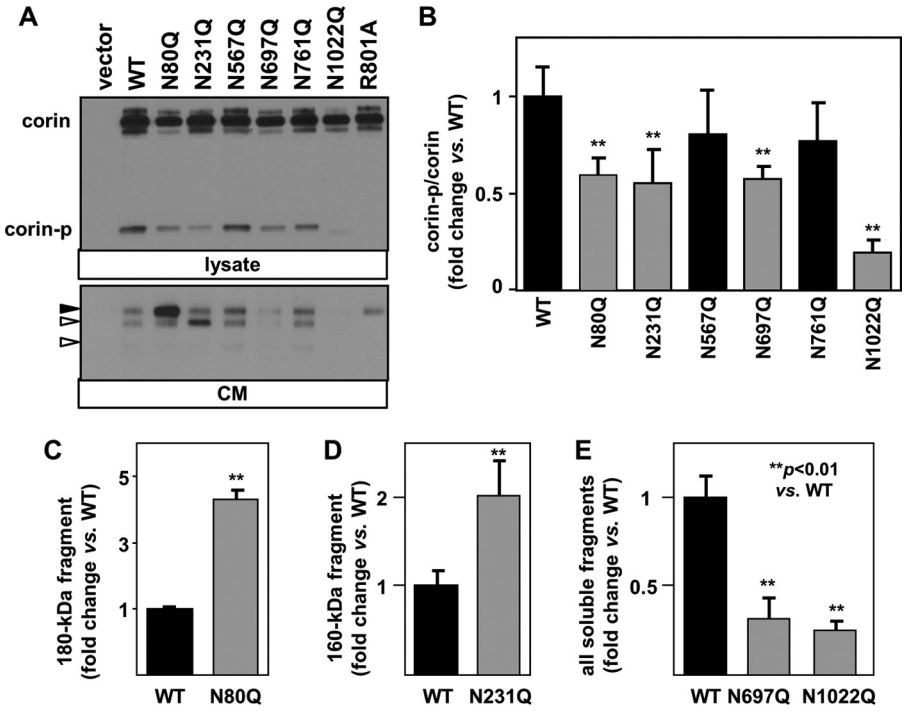

FIGURE 3. **Zymogen activation and ectodomain shedding of corin WT and *N*-glycosylation site mutants in HL-1 cardiomyocytes.** *A*, Western blotting analysis of corin zymogen activation (*top*) and ectodomain shedding (*bottom*) in the cell lysate (*lysate*) and conditioned medium (*CM*) from transfected HL-1 cells. *B*, ratios of corin-p *versus* corin bands, as estimated by densitometric analysis of Western blots. $n = 5$/group. *C*, relative levels of the ~180-kDa fragment in samples from WT and N80Q mutant. $n = 3$/group. *D*, relative levels of the ~160-kDa fragment in samples from WT and N231Q mutant. $n = 3$/group. *E*, relative levels of all three fragments in samples from WT and N697Q and N1022Q mutants. $n = 3$/group. All values are means ± S.D. (*error bars*). **, $p < 0.01$ *versus* WT in each group.

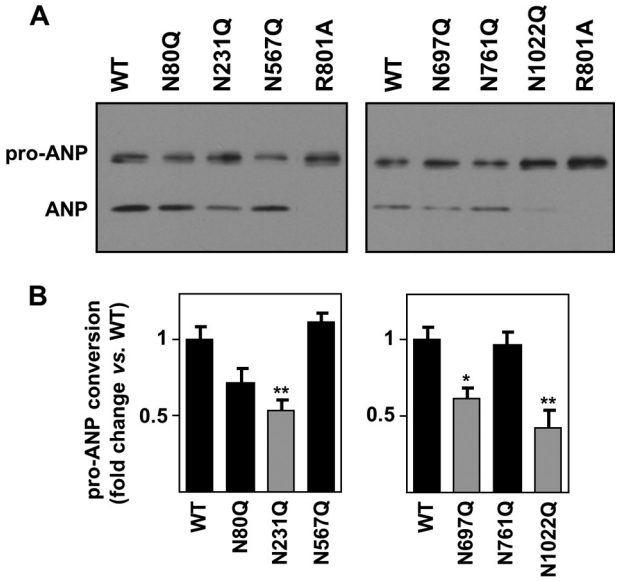

FIGURE 4. **Pro-ANP processing activity.** *A*, Western blotting analysis of pro-ANP processing by corin WT and mutants. The conditioned medium containing human pro-ANP was incubated with transfected HEK293 cells expressing corin WT and mutants. Pro-ANP and ANP fragments were analyzed by immunoprecipitation and Western blotting. *B*, relative pro-ANP processing activities of corin WT and mutants, as estimated by densitometric analysis of Western blots. Values are means ± S.D. (*error bars*). Data are representative of five independent experiments. *, $p < 0.05$; **, $p < 0.01$ *versus* WT in each group.

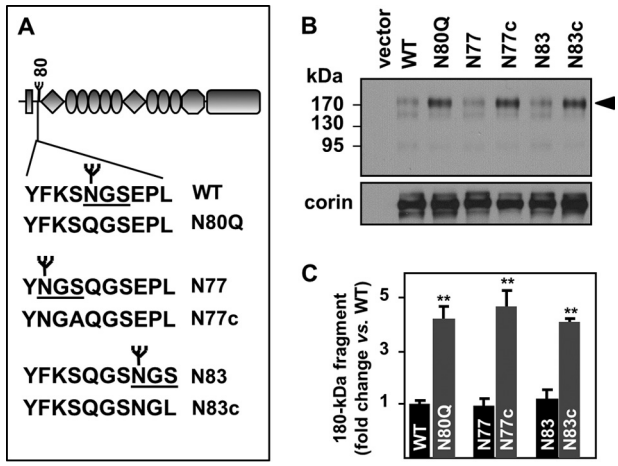

FIGURE 5. **Mutation at Asn-80 increased shedding in the juxtamembrane domain.** *A*, *N*-glycosylation site at Asn-80 and amino acid sequences of N77 and N83 mutants and respective controls. The *N*-glycosylation sequence (*NGS*) is *underlined*. *B*, Western blotting analysis of soluble corin fragments in the conditioned medium for HEK293 cells expressing corin WT and mutants (*top*). The ~180 kDa band is indicated by an *arrowhead*. Corin proteins in cell lysates were shown as a control (*bottom*). *C*, relative levels of the ~180 kDa band in WT and mutants N80Q, N77, N77c, N83, and N83c, as estimated by densitometric analysis of Western blots. Values are means ± S.D. (*error bars*) from six independent experiments. **, $p < 0.01$ *versus* WT, N77, and N83, respectively.

6*B*). To test whether the increased level of the ~160 kDa band in the N231Q mutant was due to enhanced corin autocleavage, we made a double mutant, N231Q/S985A (Fig. 6*A*), which was catalytically inactive. In Western analysis, the ~160 kDa band was not detected in the conditioned medium from S985A and N231Q/S985A mutants (Fig. 6*C*, *left*), indicating the enhanced autocleavage in N231Q mutant. In Western analysis of biotin-labeled cell surface proteins, levels of corin zymogen and the corin-p bands were lower in N231Q mutant than in WT (Fig. 6, *C* (*middle*) and *D*). Consistently, the level of the corin-p band

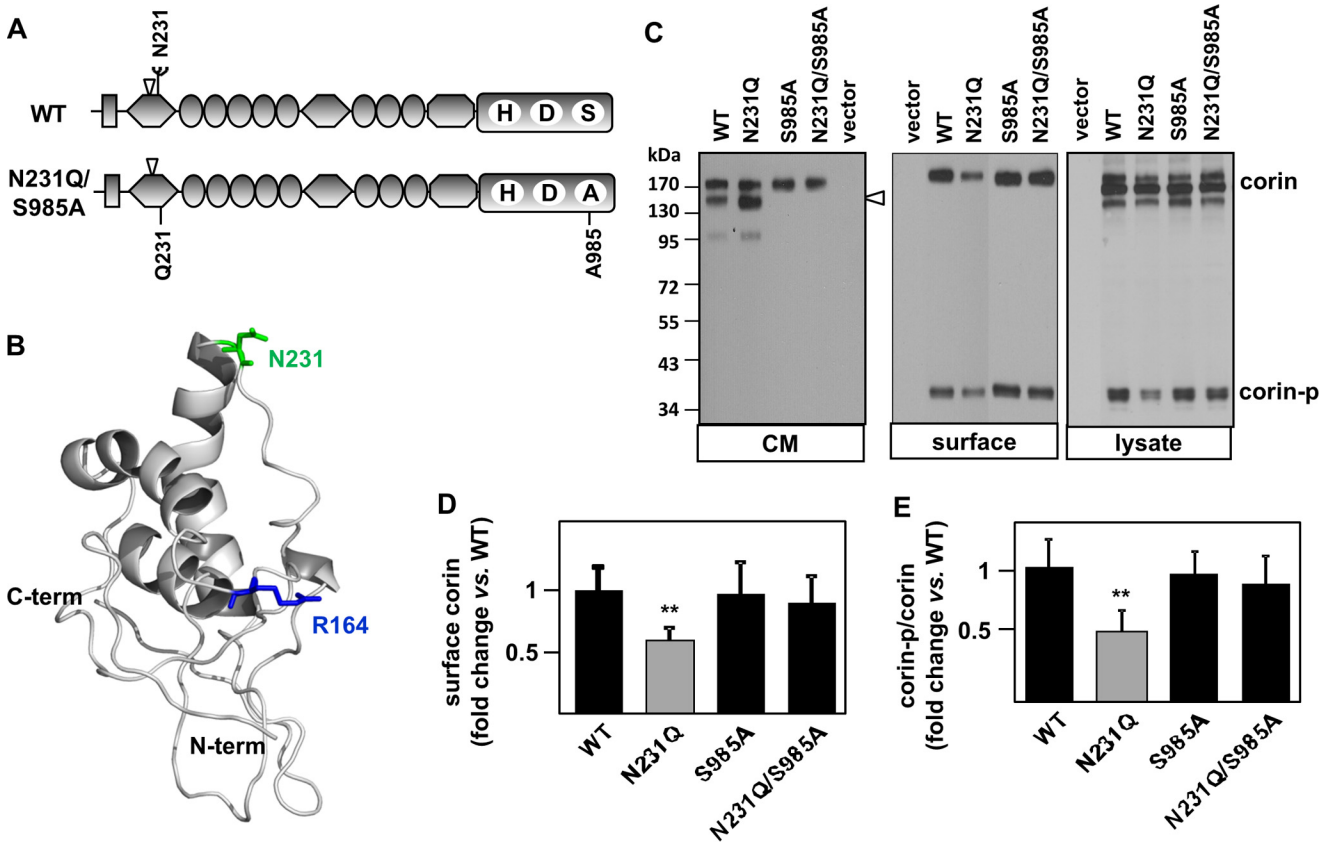

FIGURE 6. **Mutation at Asn-231 increased corin autocleavage in the Fz1 domain.** *A*, Asn-231 residue and autocleavage site in the Fz1 domain. The active sites His (*H*), Asp (*D*), and Ser (*S*) in the protease domain of WT corin are shown. In mutant N231Q/S985A, Asn-231 and Ser-985 were replaced by Gln (*Q*) and Ala (*A*), respectively. *B*, a *three-dimensional model* of the Fz1 domain of corin. Residue Asn-231 is shown in *green*. The autocleavage site residue Arg-164 is shown in *blue*. *C*, Western blotting analysis of corin fragments in the conditioned medium (*CM*), and corin proteins on the cell surface (*surface*) and in cell lysates (*lysate*) from HEK293 cells expressing WT and mutants. The ~160 kDa band is indicated by an *arrowhead* (*left panel*). The activated corin protease domain fragment is indicated (*corin-p*) (*middle* and *right panels*). In the *middle* and *right panels*, cropped sections from single full-length blots of the same experiments are used. *D*, relative levels of cell surface corin in WT and mutants. **, $p < 0.01$ *versus* WT. *E*, ratios of corin-p *versus* corin bands in WT and mutants. **, $p < 0.01$ *versus* WT. Values are means ± S.D. (*error bars*) from four independent experiments.

also was lower in N231Q mutant cell lysate compared with that in lysates from WT and mutants S985A and N231A/S985A (Fig. 6, *C* (*right*) and *E*). In contrast, corin zymogen bands in cell lysates, which represented mostly intracellular corin molecules, appeared at similar levels in WT and the mutants. The results indicate that abolishing the *N*-glycosylation site at Asn-231 increased autocleavage in the Fz1 domain, thereby reducing the corin level on the cell surface.

Reduced Cell Surface Expression of N231Q, N697Q, and N1022Q Mutants—We immunostained cell surface corin in the transfected HEK293 cells. Under membrane non-permeable conditions, positive surface staining was detected in the cells expressing WT and mutants N231Q, N697Q, and N1022Q (Fig. 7*A*). The staining appeared stronger in the cells expressing WT than in the mutants. To verify this result quantitatively, cell surface proteins were biotin-labeled and analyzed by Western blotting. Levels of cell surface corin in N231Q, N697Q, and N1022Q mutants were significantly lower at 58 ± 10, 64 ± 9, and 27 ± 8% of WT, respectively (Fig. 7, *B* and *C*). In controls, total corin levels were similar in all lysate samples (Fig. 7*B*, *bottom*). In flow cytometric analysis with intact cells, surface corin-positive cells were fewer in number in N231Q, N697Q, and N1022Q plasmid-transfected HEK293 cells compared with in WT controls (40.6 ± 5.7, 39.3 ± 7.3, and 30.2 ± 8.0%, respectively, *versus* 47.5 ± 5.9% in WT; $n \geq 8$; all p values <0.05) (Fig. 7*D*). These results show that N231Q, N697Q, and N1022Q mutant corin levels were reduced on the surface of the transfected HEK293 cells.

Importance of N-Glycosylation Site Locations in the Corin Protease Domain—In the human corin protease domain, Asn-1022 is the only predicted *N*-glycosylation site (Fig. 8*A*). The reduced N1022Q mutant levels on the cell surface and in the conditioned medium suggest that *N*-glycans in this domain are important for cell surface targeting. In rat and mouse corin proteins, the protease domain has two *N*-glycosylation sites: one corresponding to Ser-903 and the other to Asn-1022 in human corin (Fig. 8*A*) (38). To understand the spatial position of these two sites, we generated a three-dimensional model of the corin protease domain, which shows that Ser-903 and Asn-1022 residues are located in separated surface loops (Fig. 8*B*). To test whether *N*-glycosylation at either residue 903 or 1022 is sufficient for cell surface targeting, we made S903N/N1022Q and S903N mutants (Fig. 8*A*). In lysates from the transfected cells, levels of the corin-p band were similar in WT, S903N/N1022Q, and S903N mutants (Fig. 8*C*, *left*). This band in the S903N/N1022Q mutant migrated more slowly than that in the N1022Q mutant (lacking *N*-glycans) but similarly to that in WT. The band in S903N mutant migrated more slowly than

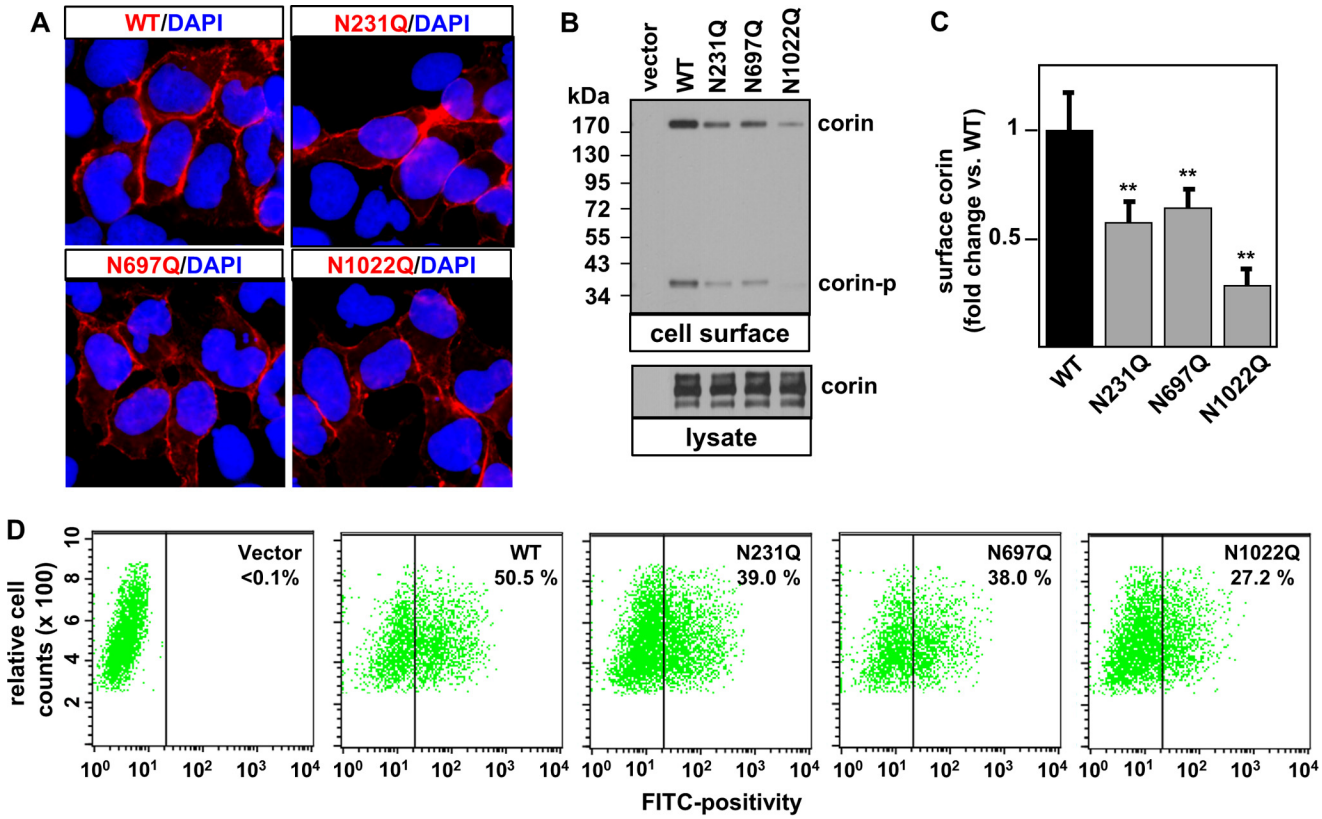

FIGURE 7. **Cell surface corin expression.** *A*, immunostaining of corin in membrane non-permeabilized HEK293 cells expressing corin WT and mutants. Corin was stained in *red*. Cell nuclei were stained by DAPI in *blue*. *B*, Western blotting analysis of biotin-labeled cell surface corin proteins in transfected HEK293 cells (*top*). Corin proteins in cell lysates were shown as a control (*bottom*). *C*, relative levels of cell surface corin in WT and mutants, as estimated by densitometric analysis of Western blots. Data are means ± S.D. (*error bars*) from four independent experiments. *, $p < 0.05$; **, $p < 0.01$ *versus* WT. *D*, flow cytometric analysis of cell surface corin in transfected HEK293 cells. Data are representative of ≥8 independent experiments. Percentages of corin-positive cells in the representative experiment are indicated.

that in WT and S903N/N1002Q mutant, probably due to more abundant *N*-glycans at both the 903 and 1022 sites. Consistently, similar migration patterns of this band were observed in WT and the mutants after glycosidase digestion (Fig. 8*C*, *right*). The results indicate that *N*-glycosylation at either residue 903 or 1022 is sufficient for efficient cell surface targeting and zymogen activation of corin in HEK293 cells.

These results led to the hypothesis that the role of *N*-glycosylation in promoting corin cell surface expression and zymogen activation may not be site-specific in the protease domain. To test this hypothesis, we designed two additional mutants, T963N/N1022Q and S975N/N1022Q, in which new *N*-glycosylation sites are created in different surface loops of the corin protease domain (Fig. 8*B*). T963N corresponds to an *N*-glycosylation site in some membrane-bound serine proteases, such as enteropeptidase (39) and spinesin (40), and S975N is in a separate surface loop (Fig. 8, *A* and *B*). In Western blotting analysis, the corin-p bands from WT and S975N/N1022Q mutant migrated similarly, whereas the band from T963N/N1022Q mutant migrated more slowly (Fig. 8*D*, *left*). The intensity of the band from the T963N/N1022Q mutant was stronger than that of WT, whereas that of the S975N/N1022Q mutant was weaker. After glycosidase digestion, the corin-p bands from WT and the mutants all migrated faster, suggesting that T963N/N1022Q and S975N/N1022Q mutants contained *N*-glycans in their protease domains and that the T963N/N1022Q mutant had more abundant *N*-glycans than did the S975N/N1022Q mutant. These results indicate that alternative *N*-glycosylation sites may be created in the corin protease domain to promote cell surface targeting and zymogen activation.

DISCUSSION

N-Glycosylation is a major post-translational modification that regulates protein folding, stability, intracellular trafficking, and protein-protein interactions (41–43). *N*-Glycans also promote membrane protein sorting in cells (44–47). Human corin has 19 predicted *N*-glycosylation sites (2), most of which are evolutionarily conserved, indicating their functional importance. Previously, we and others found that *N*-glycans were required for corin cell surface expression and activation (25–27). It was unknown, however, how *N*-glycans at different sites might regulate corin biosynthesis and processing. Here, we analyzed corin mutants, in which *N*-glycosylation sites were mutated individually. We found that removing each of the 19 *N*-glycosylation sites did not affect corin protein synthesis in the transfected HEK293 cells. Our results, however, revealed distinct roles of *N*-glycosylation at different corin sites in promoting cell surface expression and preventing ectodomain shedding.

We found that *N*-glycosylation at Asn-80 inhibited corin shedding in the juxtamembrane domain. Abolishing this site

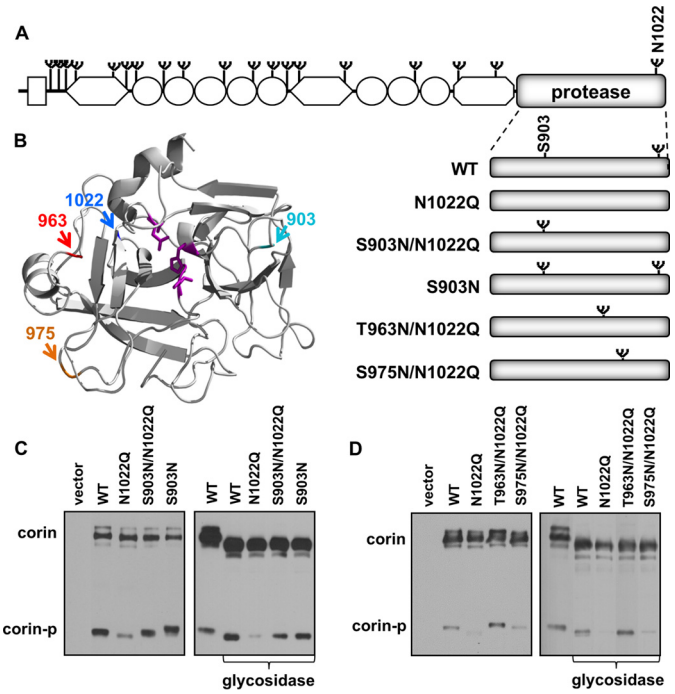

FIGURE 8. **Effects of *N*-glycosylation site mutations in the protease domain.** *A*, illustration of *N*-glycosylation sites in the protease domain of human corin WT and mutants. *B*, a *three-dimensional model* of the protease domain of human corin. The active sites His, Asp, and Ser are shown in *purple*. Residues 903, 963, 975, and 1022 that were mutated are indicated. *C*, Western blotting analysis of corin WT and mutants N1022Q, S903N/N1022Q, and S903N in cell lysates without (*left*) and with (*right*) peptide-*N*-glycosidase F (*glycosidase*) digestion. *D*, Western blotting analysis of corin WT and mutants N1022Q, T963N/N1022Q, and S975N/N1022Q in cell lysates without (*left*) and with (*right*) peptide-*N*-glycosidase F (*glycosidase*) digestion. The data are representative of at least three independent experiments.

increased the shedding of the ~180-kDa fragment (Figs. 2, 3, and 5). Previously, we showed that this fragment was cleaved by ADAM10 and that the cleavage was not sequence-specific (36), consistent with the notoriously poor substrate sequence specificity of ADAMs (48–50). We now show that the protective effect of *N*-glycosylation in this region is not position-dependent because *N*-glycosylation at residue 77, 80, or 83 had a similar protective effect (Fig. 5). In controls, no such protective effect was observed in mutants N77c and N83c, in which Asn at positions 77 and 83 was not followed by the *N*-glycosylation consensus sequence, suggesting that the protective effect in the N77 and N83 mutants was probably due to *N*-glycosylation but not the Asn residue change. These results indicate that the presence of *N*-glycans near the cell membrane is probably sufficient to create a barrier to block the ADAM10-mediated shedding. Alternatively, *N*-glycans in this region of corin may lead to a particular conformation that is unfavorable for ADAM10 recognition.

In addition to the ADAM10-mediated cleavage in the juxtamembrane domain, corin undergoes autocleavage in the Fz1 domain and LDLR5 repeat, producing fragments of ~160 and ~100 kDa, respectively (36). High levels of the ~160 kDa band in the conditioned medium from N231Q mutant (Figs. 2, 3, and 6) indicated that abolishing *N*-glycosylation at Asn-231 enhanced autocleavage in the Fz1 domain. Consistently, the band was not detected in the double mutant N231Q/S985A that lacked the catalytic activity (Fig. 6*C*). The autocleavage reduced N231Q mutant expression on the cell surface (Figs. 6 and 7). In the Fz1 domain, the Arg-164 residue has been identified as the autocleavage site (36). In a three-dimensional model based on the mouse Fz8 crystal structure (51), the distance between Asn-231 and Arg-164 was ~30 Å (Fig. 6*B*). It is unclear how *N*-glycosylation at Asn-231 may inhibit autocleavage at Arg-164 because a direct protection of Arg-164 by *N*-glycans on Asn-231 seems less likely. A possible explanation is that the presence of *N*-glycans on Asn-231 may reduce the flexibility of the Fz1 domain, thereby keeping a conformation unfavorable for autocleavage at Arg-164. In addition to Arg-164 in the Fz1 domain, Arg-427 in the LDLR5 repeat was identified as another autocleavage site, producing the ~100-kDa fragment (36). In this study, we did not observe an increased level of the ~100 kDa band in the conditioned medium from N446Q mutant (Fig. 2*A*), indicating that *N*-glycans at Asn-446 have little effect on autocleavage at the Arg-427 residue.

In N697Q and N1022Q mutants, soluble corin levels in the conditioned medium were low (Fig. 2). The reduction was not caused by impaired shedding, because mutant protein levels also were low on the cell surface (Fig. 7), suggesting that the reduction was probably caused by poor intracellular trafficking. These data indicate that *N*-glycans in the scavenger receptor and the protease domains may act as cell membrane sorting signals, facilitating corin cell surface expression. The finding of low N1022Q mutant expression on the cell surface is consistent with the previous studies with rat corin, in which removing two *N*-glycosylation sites, Asn-968 and Asn-1087, in the protease domain reduced corin cell surface expression and zymogen activation (25). Residues Asn-968 and Asn-1087 in rat corin correspond to Ser-903 and Asn-1022, respectively, in human corin (2, 38). We found that *N*-glycosylation at either position 903 or 1022 was sufficient for human corin zymogen activation (Fig. 8).

To test the importance of *N*-glycosylation site location in the protease domain in corin zymogen activation, we analyzed corin mutants with alternative *N*-glycosylation sites in the protease domain. We found that the newly created *N*-glycosylation site at position 963, corresponding to an *N*-glycosylation site in other trypsin-like proteases, such as enteropeptidase (39), spinesin (40), and HAT-like 5 (52), or at position 975 in a separate surface loop, also promoted corin zymogen activation (Fig. 8). The results indicate that *N*-glycosylation at Asn-1022 in the human corin protease domain may not have an advantage over the other possible sites. At this time, specific roles of *N*-glycans in the scavenger receptor and the protease domains of corin in facilitating intracellular trafficking and membrane targeting remain unknown. One possibility is that *N*-glycans in the C-terminal region of corin may act as sorting signals or binding elements for efficient trafficking to the cell membrane. Previously, *N*-glycosylation sites in the C-terminal protease domain of enteropeptidase (30) and matriptase (31) were shown to be critical for apical sorting and zymogen activation. Our results suggest that a similar *N*-glycan-mediated cell surface targeting mechanism may apply to the other type II transmembrane serine proteases that are involved in a variety of biological processes and diseases (33, 53, 54). In functional studies, we

showed that N80Q, N231Q, N687Q, and N1022Q mutants had reduced pro-ANP processing activity (Fig. 4). In principle, naturally occurring mutations that abolish *N*-glycosylation sites may occur in corin. Such mutations may impair the biosynthesis and function of corin and inhibit the ANP signaling pathway, which may contribute to hypertension and heart disease in patients.

Acknowledgment—We thank Nancy Fiordalisi for critical reading of the manuscript.

REFERENCES

1. Wu, Q. (2007) The serine protease corin in cardiovascular biology and disease. *Front. Biosci.* **12,** 4179–4190
2. Yan, W., Sheng, N., Seto, M., Morser, J., and Wu, Q. (1999) Corin, a mosaic transmembrane serine protease encoded by a novel cDNA from human heart. *J. Biol. Chem.* **274,** 14926–14935
3. Hooper, J. D., Scarman, A. L., Clarke, B. E., Normyle, J. F., and Antalis, T. M. (2000) Localization of the mosaic transmembrane serine protease corin to heart myocytes. *Eur J Biochem.* **267,** 6931–6937
4. Ichiki, T., Huntley, B. K., Heublein, D. M., Sandberg, S. M., McKie, P. M., Martin, F. L., Jougasaki, M., and Burnett, J. C., Jr. (2011) Corin is present in the normal human heart, kidney, and blood, with pro-B-type natriuretic peptide processing in the circulation. *Clin Chem* **57,** 40–47
5. Wu, F., Yan, W., Pan, J., Morser, J., and Wu, Q. (2002) Processing of pro-atrial natriuretic peptide by corin in cardiac myocytes. *J. Biol. Chem.* **277,** 16900–16905
6. Armaly, Z., Assady, S., and Abassi, Z. (2013) Corin: a new player in the regulation of salt-water balance and blood pressure. *Curr. Opin. Nephrol. Hypertens.* **22,** 713–722
7. Chan, J. C., Knudson, O., Wu, F., Morser, J., Dole, W. P., and Wu, Q. (2005) Hypertension in mice lacking the proatrial natriuretic peptide convertase corin. *Proc. Natl. Acad. Sci. U.S.A.* **102,** 785–790
8. Klein, J. D. (2010) Corin: an ANP protease that may regulate sodium reabsorption in nephrotic syndrome. *Kidney Int.* **78,** 635–637
9. Wu, Q., Xu-Cai, Y. O., Chen, S., and Wang, W. (2009) Corin: new insights into the natriuretic peptide system. *Kidney Int.* **75,** 142–146
10. Yan, W., Wu, F., Morser, J., and Wu, Q. (2000) Corin, a transmembrane cardiac serine protease, acts as a pro-atrial natriuretic peptide-converting enzyme. *Proc. Natl. Acad. Sci. U.S.A.* **97,** 8525–8529
11. Cannone, V., Huntley, B. K., Olson, T. M., Heublein, D. M., Scott, C. G., Bailey, K. R., Redfield, M. M., Rodeheffer, R. J., and Burnett, J. C., Jr. (2013) Atrial natriuretic peptide genetic variant rs5065 and risk for cardiovascular disease in the general community: a 9-year follow-up study. *Hypertension* **62,** 860–865
12. Dong, N., Fang, C., Jiang, Y., Zhou, T., Liu, M., Zhou, J., Shen, J., Fukuda, K., Qin, J., and Wu, Q. (2013) Corin mutation R539C from hypertensive patients impairs zymogen activation and generates an inactive alternative ectodomain fragment. *J. Biol. Chem.* **288,** 7867–7874
13. Dries, D. L., Victor, R. G., Rame, J. E., Cooper, R. S., Wu, X., Zhu, X., Leonard, D., Ho, S. I., Wu, Q., Post, W., and Drazner, M. H. (2005) Corin gene minor allele defined by 2 missense mutations is common in blacks and associated with high blood pressure and hypertension. *Circulation* **112,** 2403–2410
14. Hodgson-Zingman, D. M., Karst, M. L., Zingman, L. V., Heublein, D. M., Darbar, D., Herron, K. J., Ballew, J. D., de Andrade, M., Burnett, J. C., Jr., and Olson, T. M. (2008) Atrial natriuretic peptide frameshift mutation in familial atrial fibrillation. *N. Engl. J. Med.* **359,** 158–165
15. Lynch, A. I., Claas, S. A., and Arnett, D. K. (2009) A review of the role of atrial natriuretic peptide gene polymorphisms in hypertension and its sequelae. *Curr. Hypertens. Rep.* **11,** 35–42
16. Rame, J. E., Drazner, M. H., Post, W., Peshock, R., Lima, J., Cooper, R. S., and Dries, D. L. (2007) Corin I555(P568) allele is associated with enhanced cardiac hypertrophic response to increased systemic afterload. *Hypertension* **49,** 857–864
17. Rubattu, S., Sciarretta, S., and Volpe, M. (2014) Atrial natriuretic peptide gene variants and circulating levels: implications in cardiovascular diseases. *Clin. Sci.* **127,** 1–13
18. Sciarretta, S., Marchitti, S., Bianchi, F., Moyes, A., Barbato, E., Di Castro, S., Stanzione, R., Cotugno, M., Castello, L., Calvieri, C., Eberini, I., Sadoshima, J., Hobbs, A. J., Volpe, M., and Rubattu, S. (2013) C2238 atrial natriuretic peptide molecular variant is associated with endothelial damage and dysfunction through natriuretic peptide receptor C signaling. *Circ. Res.* **112,** 1355–1364
19. Zhou, Y., and Wu, Q. (2014) Corin in natriuretic peptide processing and hypertension. *Curr. Hypertens. Rep.* **16,** 415
20. Armstrong, D. W., Tse, M. Y., O'Tierney-Ginn, P. F., Wong, P. G., Ventura, N. M., Janzen-Pang, J. J., Matangi, M. F., Johri, A. M., Croy, B. A., Adams, M. A., and Pang, S. C. (2013) Gestational hypertension in atrial natriuretic peptide knockout mice and the developmental origins of salt-sensitivity and cardiac hypertrophy. *Regul. Pept.* **186,** 108–115
21. Cui, Y., Wang, W., Dong, N., Lou, J., Srinivasan, D. K., Cheng, W., Huang, X., Liu, M., Fang, C., Peng, J., Chen, S., Wu, S., Liu, Z., Dong, L., Zhou, Y., and Wu, Q. (2012) Role of corin in trophoblast invasion and uterine spiral artery remodelling in pregnancy. *Nature* **484,** 246–250
22. Kaitu'u-Lino, T. J., Ye, L., Tuohey, L., Dimitriadis, E., Bulmer, J., Rogers, P., Menkhorst, E., Van Sinderen, M., Girling, J. E., Hannan, N., and Tong, S. (2013) Corin, an enzyme with a putative role in spiral artery remodeling, is up-regulated in late secretory endometrium and first trimester decidua. *Hum. Reprod.* **28,** 1172–1180
23. Zhou, Y., and Wu, Q. (2013) Role of corin and atrial natriuretic peptide in preeclampsia. *Placenta* **34,** 89–94
24. Dong, N., Zhou, T., Zhang, Y., Liu, M., Li, H., Huang, X., Liu, Z., Wu, Y., Fukuda, K., Qin, J., and Wu, Q. (2014) Corin mutations K317E and S472G from preeclamptic patients alter zymogen activation and cell surface targeting. *J. Biol. Chem.* **289,** 17909–17916
25. Liao, X., Wang, W., Chen, S., and Wu, Q. (2007) Role of glycosylation in corin zymogen activation. *J. Biol. Chem.* **282,** 27728–27735
26. Qi, X., Jiang, J., Zhu, M., and Wu, Q. (2011) Human corin isoforms with different cytoplasmic tails that alter cell surface targeting. *J. Biol. Chem.* **286,** 20963–20969
27. Gladysheva, I. P., King, S. M., and Houng, A. K. (2008) *N*-Glycosylation modulates the cell-surface expression and catalytic activity of corin. *Biochem. Biophys. Res. Commun.* **373,** 130–135
28. Gladysheva, I. P., Robinson, B. R., Houng, A. K., Kováts, T., and King, S. M. (2008) Corin is co-expressed with pro-ANP and localized on the cardiomyocyte surface in both zymogen and catalytically active forms. *J. Mol. Cell Cardiol.* **44,** 131–142
29. Ichiki, T., Boerrigter, G., Huntley, B. K., Sangaralingham, S. J., McKie, P. M., Harty, G. J., Harders, G. E., and Burnett, J. C., Jr. (2013) Differential expression of the pro-natriuretic peptide convertases corin and furin in experimental heart failure and atrial fibrosis. *Am. J. Physiol. Regul. Integr. Comp. Physiol.* **304,** R102–R109
30. Zheng, X., Lu, D., and Sadler, J. E. (1999) Apical sorting of bovine enteropeptidase does not involve detergent-resistant association with sphingolipid-cholesterol rafts. *J. Biol. Chem.* **274,** 1596–1605
31. Oberst, M. D., Williams, C. A., Dickson, R. B., Johnson, M. D., and Lin, C. Y. (2003) The activation of matriptase requires its noncatalytic domains, serine protease domain, and its cognate inhibitor. *J. Biol. Chem.* **278,** 26773–26779
32. Jiang, J., Yang, J., Feng, P., Zuo, B., Dong, N., Wu, Q., and He, Y. (2014) N-glycosylation is required for matriptase-2 autoactivation and ectodomain shedding. *J. Biol. Chem.* **289,** 19500–19507
33. Antalis, T. M., Bugge, T. H., and Wu, Q. (2011) Membrane-anchored serine proteases in health and disease. *Prog. Mol. Biol. Transl. Sci.* **99,** 1–50
34. Miller, G. S., and List, K. (2013) The matriptase-prostasin proteolytic cascade in epithelial development and pathology. *Cell Tissue Res.* **351,** 245–253
35. Claycomb, W. C., Lanson, N. A., Jr., Stallworth, B. S., Egeland, D. B., Delcarpio, J. B., Bahinski, A., and Izzo, N. J., Jr. (1998) HL-1 cells: a cardiac muscle cell line that contracts and retains phenotypic characteristics of the adult cardiomyocyte. *Proc. Natl. Acad. Sci. U.S.A.* **95,** 2979–2984
36. Jiang, J., Wu, S., Wang, W., Chen, S., Peng, J., Zhang, X., and Wu, Q. (2011)

Ectodomain shedding and autocleavage of the cardiac membrane protease corin. *J. Biol. Chem.* **286,** 10066–10072
37. Schwede, T., Kopp, J., Guex, N., and Peitsch, M. C. (2003) SWISS-MODEL: an automated protein homology-modeling server. *Nucleic Acids Res.* **31,** 3381–3385
38. Langenickel, T. H., Pagel, I., Buttgereit, J., Tenner, K., Lindner, M., Dietz, R., Willenbrock, R., and Bader, M. (2004) Rat corin gene: molecular cloning and reduced expression in experimental heart failure. *Am. J. Physiol. Heart Circ. Physiol.* **287,** H1516–H1521
39. Kitamoto, Y., Yuan, X., Wu, Q., McCourt, D. W., and Sadler, J. E. (1994) Enterokinase, the initiator of intestinal digestion, is a mosaic protease composed of a distinctive assortment of domains. *Proc. Natl. Acad. Sci. U.S.A.* **91,** 7588–7592
40. Yamaguchi, N., Okui, A., Yamada, T., Nakazato, H., and Mitsui, S. (2002) Spinesin/TMPRSS5, a novel transmembrane serine protease, cloned from human spinal cord. *J. Biol. Chem.* **277,** 6806–6812
41. Dalziel, M., Crispin, M., Scanlan, C. N., Zitzmann, N., and Dwek, R. A. (2014) Emerging principles for the therapeutic exploitation of glycosylation. *Science* **343,** 1235681
42. Hart, G. W., and Copeland, R. J. (2010) Glycomics hits the big time. *Cell* **143,** 672–676
43. Moremen, K. W., Tiemeyer, M., and Nairn, A. V. (2012) Vertebrate protein glycosylation: diversity, synthesis and function. *Nat. Rev. Mol. Cell Biol.* **13,** 448–462
44. Haga, Y., Ishii, K., and Suzuki, T. (2011) *N*-Glycosylation is critical for the stability and intracellular trafficking of glucose transporter GLUT4. *J. Biol. Chem.* **286,** 31320–31327
45. Martínez-Maza, R., Poyatos, I., López-Corcuera, B., Núñez, E., Giménez, C., Zafra, F., and Aragón, C. (2001) The role of *N*-glycosylation in transport to the plasma membrane and sorting of the neuronal glycine transporter GLYT2. *J. Biol. Chem.* **276,** 2168–2173
46. Vagin, O., Kraut, J. A., and Sachs, G. (2009) Role of *N*-glycosylation in trafficking of apical membrane proteins in epithelia. *Am. J. Physiol. Renal Physiol.* **296,** F459–F469
47. Zhou, F., Xu, W., Hong, M., Pan, Z., Sinko, P. J., Ma, J., and You, G. (2005) The role of *N*-linked glycosylation in protein folding, membrane targeting, and substrate binding of human organic anion transporter hOAT4. *Mol. Pharmacol.* **67,** 868–876
48. Blobel, C. P. (2005) ADAMs: key components in EGFR signalling and development. *Nat. Rev. Mol. Cell Biol.* **6,** 32–43
49. Reiss, K., and Saftig, P. (2009) The "a disintegrin and metalloprotease" (ADAM) family of sheddases: physiological and cellular functions. *Semin. Cell Dev. Biol.* **20,** 126–137
50. Schlöndorff, J., and Blobel, C. P. (1999) Metalloprotease-disintegrins: modular proteins capable of promoting cell-cell interactions and triggering signals by protein-ectodomain shedding. *J. Cell Sci.* **112,** 3603–3617
51. Dann, C. E., Hsieh, J. C., Rattner, A., Sharma, D., Nathans, J., and Leahy, D. J. (2001) Insights into Wnt binding and signalling from the structures of two Frizzled cysteine-rich domains. *Nature* **412,** 86–90
52. Bugge, T. H., Antalis, T. M., and Wu, Q. (2009) Type II transmembrane serine proteases. *J. Biol. Chem.* **284,** 23177–23181
53. Szabo, R., and Bugge, T. H. (2011) Membrane-anchored serine proteases in vertebrate cell and developmental biology. *Annu. Rev. Cell Dev. Biol.* **27,** 213–235
54. Webb, S. L., Sanders, A. J., Mason, M. D., and Jiang, W. G. (2011) Type II transmembrane serine protease (TTSP) deregulation in cancer. *Front. Biosci.* (*Landmark Ed.*) **16,** 539–552